

The ANC for $^{15}\text{C} \leftrightarrow ^{14}\text{C}+n$ and the astrophysical $^{14}\text{C}(n,\gamma)^{15}\text{C}$ rate

M. McCleskey, A.M. Mukhamedzhanov, L. Trache, R.E. Tribble, V. Goldberg, Y.-W. Lui,
B. Roeder, E. Simmons, A. Spiridon, and F. Carstoiu¹
¹*IFIN-HH, Bucharest, Romania,*

The motivation for determining the asymptotic normalization coefficient (ANC) for $^{15}\text{C} \leftrightarrow ^{14}\text{C}+n$ is two fold. First, the ANC has been used to determine the astrophysically important $^{14}\text{C}(n,\gamma)^{15}\text{C}$ rate. Second, it was used in the evaluation of a method proposed to determine spectroscopic factors utilizing the ANC [1]. All of the experiments were conducted at Texas A&M Cyclotron Institute (TAMU-CI) and have been described in previous reports ([2,3]).

Determination of the ANC

The ANC is the normalization of the tail of the overlap function at large radii. This value is useful in the calculation of rates for peripheral reactions, where the largest contribution to the reaction cross section comes from these large distances. The ANC, C , is defined as

$$I_{Ax(nlj)}^B(r) \stackrel{r>R}{\approx} C_{Ax(nlj)}^B \frac{W_{\eta_B, l_B + 1/2}(2\kappa_B r)}{r} \quad (1)$$

for a reaction $A(a,b)B$ where $B=A+x$ and $b=a-x$. nlj are the quantum numbers describing the state to which nucleon n is transferred. I is the nuclear overlap function and W is a Whittaker function. This leads to a parameterization of the cross section of a peripheral reaction in terms of the ANCs [4],

$$\frac{d\sigma}{d\Omega} = \sum_{j_B l_B} (C_{Ax l_B j_B}^B)^2 (C_{bx l_a j_a}^a)^2 \frac{\sigma_{l_B j_B l_a j_a}^{DW}}{b_{Ax l_B j_B}^2 b_{bx l_a j_a}^2} \quad (2)$$

Here DW is the calculated DWBA cross section and l and j are orbital angular momentum and its projection respectively. To find the ANC for $^{15}\text{C} \leftrightarrow ^{14}\text{C}+n$ a peripheral reaction for which the other ANC of Eq. (2) is known is required. Two such reactions were utilized. First, (d,p) on ^{14}C in both forward and inverse kinematics (for the deuteron $C_{pn}^d = 0.88 \text{ fm}^{-1/2}$) and second, the heavy ion (HI) reaction $^{13}\text{C}(^{14}\text{C}, ^{15}\text{C})^{12}\text{C}$. For $^{13}\text{C}(^{14}\text{C}, ^{15}\text{C})^{12}\text{C}$, the ANC for $^{13}\text{C} \leftrightarrow ^{12}\text{C}+n$ is needed and the value of $C^2 = 2.31 \pm 0.08 \text{ fm}^{-1}$ was measured before [5].

a. HI transfer $^{13}\text{C}(^{14}\text{C}, ^{15}\text{C})^{12}\text{C}$

This reaction was performed with an incident ^{14}C energy of 12 MeV/nucleon and reaction products were measured using the MDM spectrometer and the Oxford detector. Elastic scattering was measured at the same time as the transfer and was used in the search for an acceptable optical model potential (OMP) to be used in the calculation of σ^{DW} . Two different approaches were employed, one using a grid search in real potential depth and the second based on a semi-microscopic double folding calculation [6]. For the grid search a potential with real and imaginary parts was assumed,

$$U_{OMP} = V + iW, \quad (3)$$

where V and W are of the Wood-Saxon (WS) form

$$V_{WS} = -\frac{V_0}{1 + \exp\left(\frac{r - R_0}{a_0}\right)} \quad (4)$$

For each value of V_0 , the real potential depth, the remaining five parameters were fit to reproduce the elastic scattering data. The potential was found to be continuously ambiguous, with a wide range of values of V_0 producing good fits. Because of this, five values were arbitrarily selected and the results of these are shown on the left in Fig. 1, and the values found are given in Table I. The transfer angular distributions calculated with these are shown on the right in Fig. 1 along with the measured distribution.

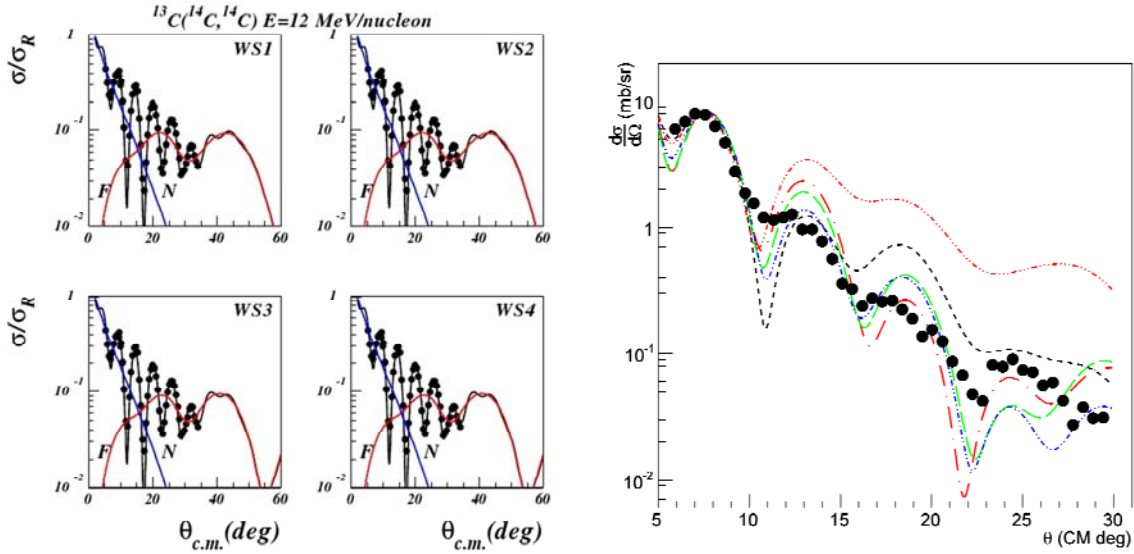


FIG. 1. On the left is the elastic scattering measurement (black dots) plotted with the results scattering calculation using the OMPs resulting from the grid search (black line). Red and Blue lines are the near/far decomposition. On the right is the DWBA calculation for the neutron transfer plotted along with the measured transfer distribution.

Table I. Optical model potential parameters for 12 MeV/nucleon ^{14}C elastic on ^{13}C .

	V (MeV)	W (MeV)	r_v (fm)	r_w (fm)	a_v (fm)	a_w (fm)	χ^2	J_v (MeV fm^3)	R_v (fm)	J_w (MeV fm^3)	R_w (fm)
WS1	77.1	13.32	0.987	1.209	0.703	0.723	3.09	225	4.480	68	5.206
WS2	118.7	14.15	0.927	1.191	0.690	0.739	3.4	292	4.275	69	5.182
WS3	162.4	15.03	0.891	1.169	0.674	0.767	3.59	357	4.132	71	5.169
WS4	203.1	16.04	0.894	1.133	0.627	0.825	3.6	438	4.038	71	5.183
WS5	248.8	16.66	0.885	1.115	0.606	0.848	3.65	516	3.965	72	5.180
DF	141.43	45.72	0.735	0.812	0.920	1.020	3.4				

The second approach to finding an OMP, the double folding calculation using the JLM effective interaction, utilized the optimal normalizations and ranges from [6]. These were four parameters were varied, but the best fit to the elastic scattering data was found with the values from [6]. The results are shown in Fig. 2 and the potential is given in Table I.

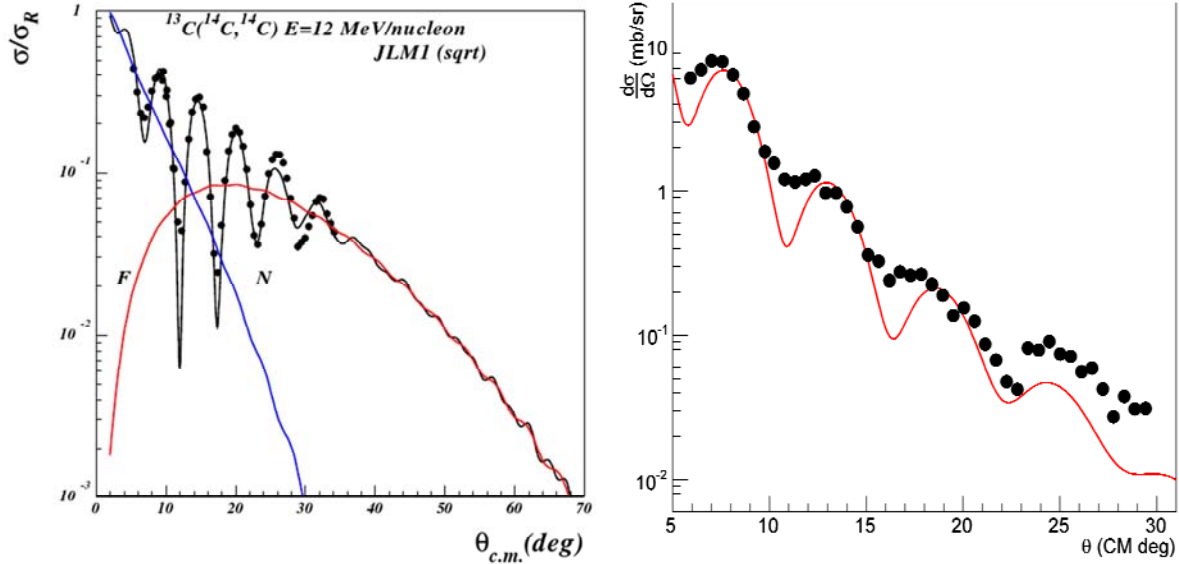


FIG. 2. On the left is the elastic scattering measurement (black dots) plotted with the results scattering calculation using the OMPs resulting from the double folding calculation (black line). Red and Blue lines are the near/far decomposition. On the right is the DWBA calculation for the neutron transfer utilizing this potential plotted along with the measured transfer distribution.

A summary of the ANCs obtained using these different DWBA calculations is given in Table II. The average value was $C^2=2.09\pm0.29 \text{ fm}^{-1}$ for transfer to the ground state, and $C^2=4.48\pm0.58\times10^{-3} \text{ fm}^{-1}$ for transfer to the 1st excited state.

Table II. Phenomenological SFs and ANCs obtained with DWBA calculation using the WS OMP fits.

	SF _{2s1/2}	$C^2_{2s1/2} \text{ (fm}^{-1}\text{)}$	SF _{1d5/2}	$C^2_{1d5/2} \times 10^{-3} \text{ (fm}^{-1}\text{)}$
WS1-WS1	1.22	2.30	1.13	4.45
WS2-WS2	1.16	2.18	1.02	4.03
WS3-WS3	1.04	1.95	1.13	4.46
WS4-WS4	0.98	1.83	1.20	4.74
WS5-WS5	1.14	2.14	1.25	4.94
DF	1.15	2.16	1.09	4.28
Average	1.12	2.09	1.14	4.48

b. Analysis of the $d(^{14}\text{C},p)^{15}\text{C}$ measurement

The inverse kinematics (d,p) on ^{14}C was measured using the Texas A&M Edinburg Catania silicon array (TECSA) [7] at TAMU-CI. A beam of 11.7 MeV/nucleon ^{14}C impinged on a $251 \pm 5 \mu\text{g}/\text{cm}^2$ CD_2 target and reaction products were measured in the backwards (lab) direction using the array of Micron YY1 detectors. The angular distributions were calculated using the code FRESKO [8]. The adiabatic distorted wave approximation (ADWA) [9] was used for the entrance channel utilizing CH89 [10] single nucleon potentials for the proton and neutron evaluated at half the deuteron energy. The finite range correction described in [11] was applied to the potential for the entrance channel. The experimental and renormalized calculations are shown in Figure 3. The ANC for the ground state was found to be $C_{2s_{1/2}}^2 = 2.01 \pm 0.24 \text{ fm}^{-1}$ and the first excited state $C_{1d_{5/2}}^2 = (4.06 \pm 0.49) \cdot 10^{-3} \text{ fm}^{-1}$, consistent with that found from $^{13}\text{C}(^{14}\text{C},^{15}\text{C})^{12}\text{C}$.

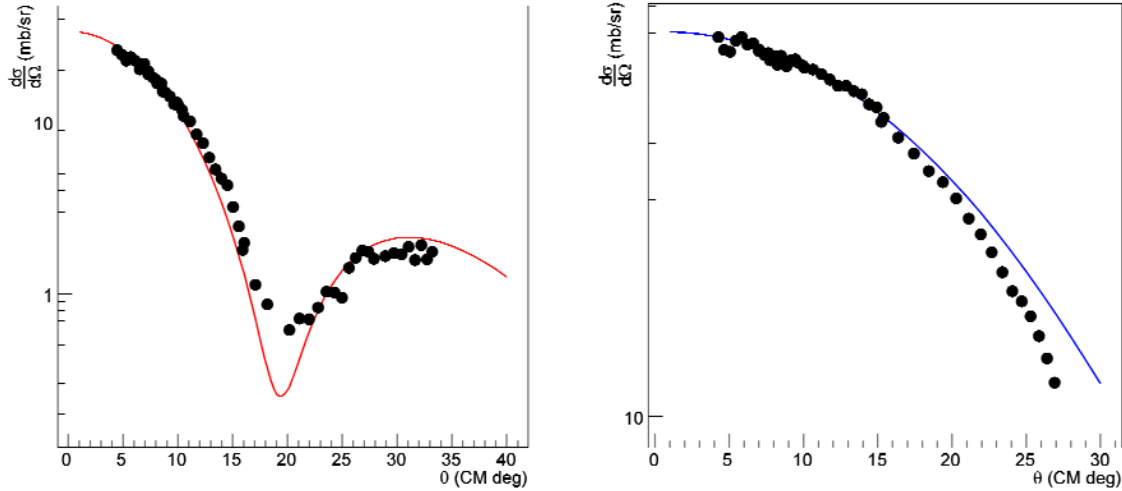


FIG. 3. On the left is the transfer to the $2s_{1/2}$ ground state. Black dots mark the experimental data points and the red line is the ADWA calculation. On the right is the 740 keV $1d_{5/2}$ first excited state, with experimental points shown as black dots and the ADWA calculation as a blue line.

c. $^{14}\text{C}(d,p)^{15}\text{C}$

The forward kinematics (d,p) on ^{14}C was measured at TAMU-CI with an incident deuteron energy of 60 MeV. As was the case in the measurement of $^{13}\text{C}(^{14}\text{C},^{15}\text{C})^{12}\text{C}$, the MDM spectrometer and Oxford detector were used. This experiment was described in [2], and only the new results from the analysis of the transfer will be presented here. The measurement of this reaction was motivated by the desire to evaluate the method outlined in [1] to determine SFs using ANCs, which will be discussed in the next section. Because of this motivation the deuteron energy of 60 MeV was selected in the hope of making this reaction non-peripheral, which would make it inappropriate for extracting the ANC.

However, the reaction turned out to be more peripheral than anticipated and as a result could be used to extract the ANC for transfer of a neutron to the ground state of ^{15}C .

The angular distribution for the transfer was calculated using the ADWA as described in the previous case of $d(^{14}\text{C},p)^{15}\text{C}$. CH89 potentials were again employed and the results are shown in Fig. 4, plotted against the experimental data. Both the ground state and first excited states are shown, however, only transfer to the ground state was sufficiently peripheral to satisfactorily extract the ANC, which was found to be $C^2=1.76\pm 0.29 \text{ fm}^{-1}$. A summary of the ANCs found from the three reactions presented here is given in Table III. The weighted average value was $1.96\pm 0.16 \text{ fm}^{-1}$ for the ground state and $4.23\pm 0.38 \cdot 10^{-3} \text{ fm}^{-1}$ for the first excited state.

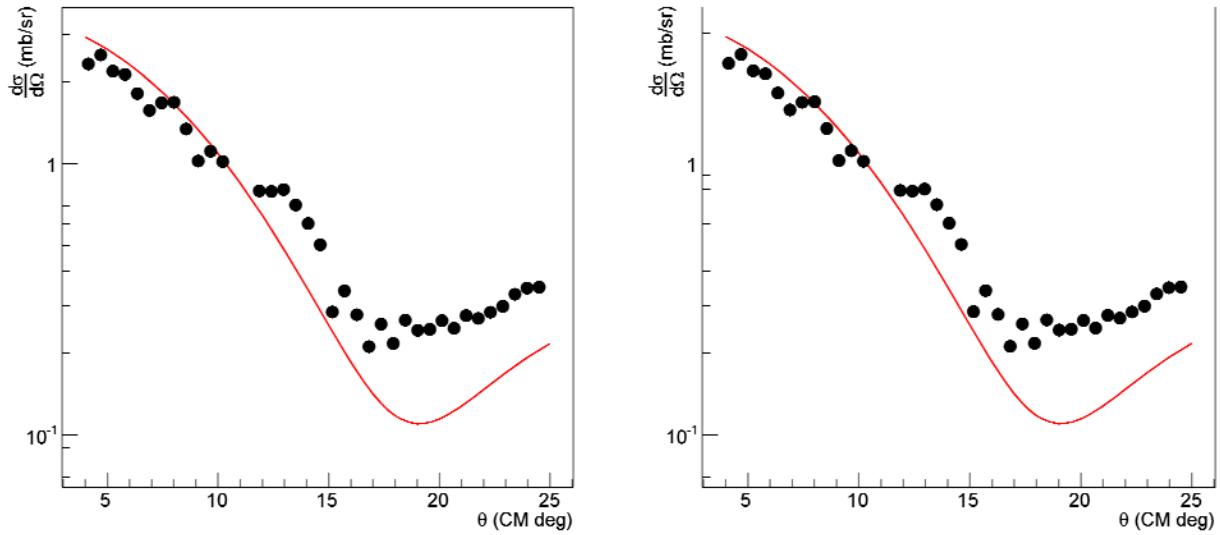


FIG. 4. On the left is the angular distribution for $^{14}\text{C}(d,p)^{15}\text{C}$ transfer to the ground state (black dots) and the ADWA calculation (red), the same is shown on the right for transfer to the $d_{5/2}$ excited state (black dots- experiment, green line ADWA).

Table III. Summary of ANCs found in the different measurements.

experiment	$C_{2s_{1/2}}^2 \text{ (fm}^{-1}\text{)}$	$C_{1d_{5/2}}^2 \text{ (fm}^{-1}\text{)}$
HI transfer	2.09 ± 0.29	$(4.48\pm 0.58)\cdot 10^{-3}$
TECSA $d(^{14}\text{C},p)^{15}\text{C}$	2.01 ± 0.24	$(4.06\pm 0.49)\cdot 10^{-3}$
60 MeV (d,p)	1.76 ± 0.29	
average	1.96 ± 0.16	$(4.23\pm 0.38)\cdot 10^{-3}$

Evaluation of a new method to extract SFs

In [1] a new method to extract SFs which used the ANC to experimentally fix the single particle ANC (SPANC) was presented. To do this a function

$$R^{DW}(b_{nlj}) = \left| \frac{\tilde{T}_{int}}{b_{nlj}} + \tilde{T}_{ext} \right|^2 \quad (5)$$

was defined where T stands for the transfer matrix element, and b is the SPANC. The transfer matrix element has been split into two parts, one which is integrated over the interior region (\tilde{T}_{int}) and is dependent on the SPANC and another \tilde{T}_{ext} which is integrated over the exterior and is not dependent on the SPANC. For a peripheral reaction, (\tilde{T}_{int}) is, by definition, negligibly small and R and thus the cross section is determined by \tilde{T}_{ext} . However, if a reaction has a non-negligible interior contribution, comparison of Eq. (5) to its experimental counterpart

$$R^{exp} = \frac{d\sigma^{exp}}{C_{lj}^2} \quad (6)$$

will fix the SPANC. This can then be used to calculate the SF using the relation

$$SF_{nlj} = \frac{C_{nlj}^2}{b_{nlj}^2} \quad (7)$$

Note that this procedure requires both a peripheral reaction to determine the ANC, and then a second, non-peripheral reaction to get the SF. R^{DW} is plotted against R^{exp} the 60 MeV $^{14}\text{C}(d,p)^{15}\text{C}$ reaction for both transfer to the ground state and first excited state in Fig.5. As can be seen, the uncertainties overlap for the entire range of SPANCs (which was varied by changing the radius parameter of the neutron binding potential which is the value plotted) for the ground state. Therefore, no information about the SF for

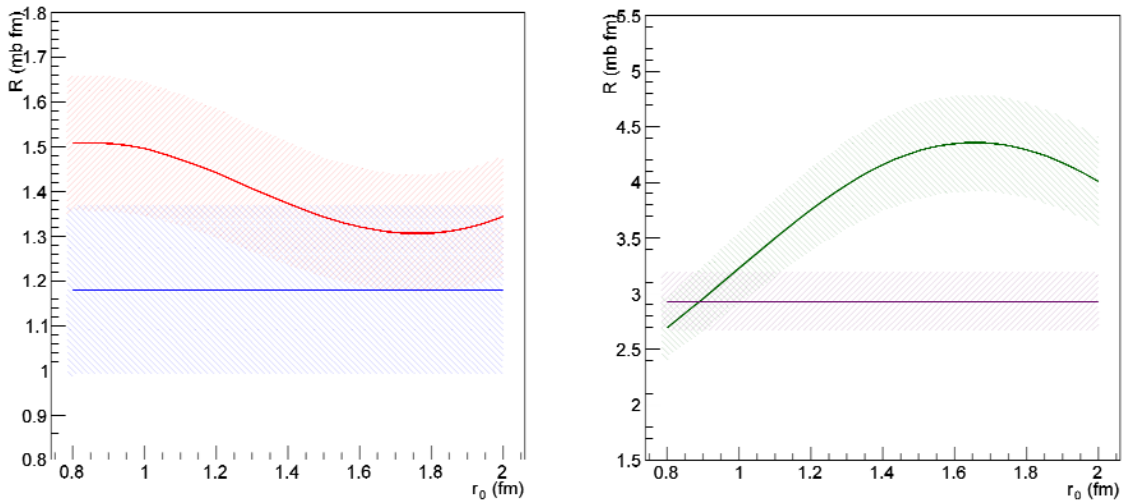


FIG. 5. R_{DW} (red) and R_{exp} (blue) for transfer to the ground state (left) and the $d_{5/2}$ first excited state (R_{DW} green, R_{exp} purple) (right). The uncertainties are shown by the hatched areas. In the calculation this is taken to be 10% and reflects the systematic uncertainty.

transfer to the ground state could be obtained for this reaction. In the plot for the first excited state, the two lines diverge around r_0 of ~ 1.15 fm, which corresponds to $b^2 = 4.01 \cdot 10^{-3} \text{ fm}^{-1}$. Using Eq. (7) one obtains a lower limit of $SF=1.05$. This is consistent with the expected single particle structure of ^{15}C . In summary, this test case highlights a significant problem with this method, namely, finding a reaction that is sufficiently non-peripheral to have a very strong dependence on the choice of SPANC, but that is still described well in the DWBA or ADWA.

Astrophysical $^{14}\text{C}(n,\gamma)^{15}\text{C}$ rate

The radiative neutron capture rates for $^{14}\text{C}(n,\gamma)^{15}\text{C}$ have been calculated using the code RADCAP [12] and the ANCs that were found in this work. At astrophysical energies only the first two states, the $2s_{1/2}$ ground state and the 740 keV $1d_{5/2}$ first excited state, contribute to the neutron capture cross section. The next state at 3.1 MeV and ~ 40 keV in width is too high to contribute [13]. S-wave neutron capture is not significant for the $^{14}\text{C}(n,\gamma)$ reaction due to parity conservation [14]. ^{14}C has $J^\pi=0^+$ and coupled with an s-wave neutron would give a system with $J^\pi=1/2^+$. Because the ground and first excited states in ^{15}C are $J^\pi=1/2^+$ and $J^\pi=5/2^+$, respectively this only allows for weak M1 and E2 transitions. Alternatively, a p-wave neutron would give the $^{14}\text{C}+n$ system $J^\pi=1/2^-$ or $3/2^-$, which would then be able to allow E1 transitions and thus a much higher cross section. For the first excited state E2 transitions should also be taken into account [14].

The neutron binding potential used was of the WS form with the real potential depth adjusted to reproduce the neutron binding energy for each state. The binding potential parameters were, for the ground state, $V_0=-54.71$ MeV, $r=2.8922$ fm, $a=0.60$ fm and $V_{SO}=-9.30$ MeV (using the SO convention described in [12]). The same geometry was used for the real and SO parts of the potential. The real depth was $V_0=-54.11$ MeV for the first excited state.

The cross section divided by the square root of the energy is given in Figure 6 for both capture to the ground state and the first excited state. The capture to the first excited state accounts for about 4% of the total (only the two states are considered). The sum of the two states is shown along with the recent direct measurement of Reifarth *et al.* [15] in Fig. 6.

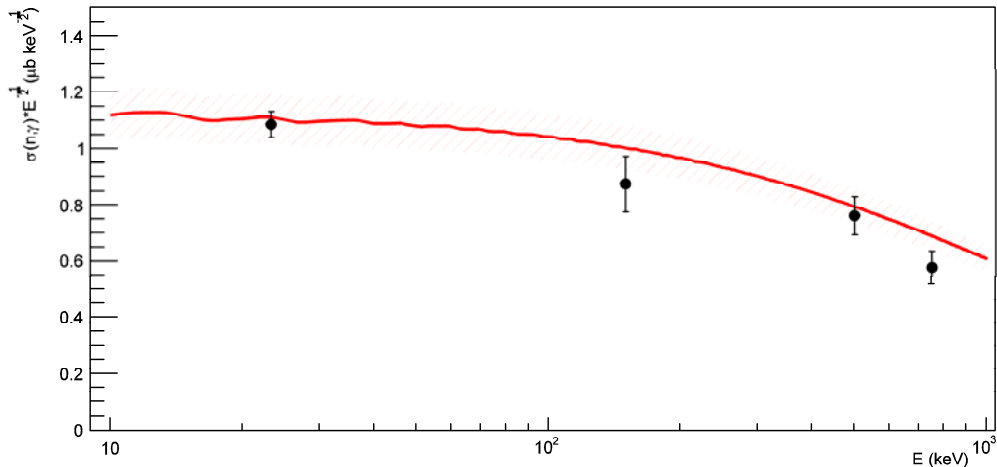


FIG. 6. Calculated cross section (sum of capture to gs and 1st exc. state, blue dots with red uncertainty) compared with Ref. [15] (black squares).

The calculated value for the cross section for capture to the ground state at 23 keV was $\sigma_{gs}(23 \text{ keV})=5.1\pm 0.4 \text{ } \mu\text{b}$ and to the first excited state was $\sigma_{exc}(23 \text{ keV})=0.19\pm 0.02 \text{ } \mu\text{b}$. The total cross section at 23 keV was found to be $\sigma(23 \text{ keV})=5.3\pm 0.5 \text{ } \mu\text{b}$, which is in good agreement with the most recent direct measurement [15].

Summary

The ANC for $^{15}\text{C}\leftrightarrow^{14}\text{C}+n$ has been determined for both the ground state and first excited state. The average values are $1.96\pm 0.16 \text{ fm}^{-1}$ for the ground state and $4.23\pm 0.38\cdot 10^{-3} \text{ fm}^{-1}$ for the first excited state. This was done as part of an effort to evaluate the new method of [1] to determine SFs with less uncertainty. The new method was found to not work at all for the GS due to a weak dependence on the neutron binding potential geometry and thus on the interior portion of the transfer matrix element for the non-peripheral reaction measured. The astrophysical $^{14}\text{C}(n,\gamma)$ rate was calculated using the determined ANCs and was found to be $\sigma(23 \text{ keV})=5.3\pm 0.5 \text{ } \mu\text{b}$, which is in good agreement with the most recent direct measurement.

- [1] A.M. Mukhamedzhanov and F.M. Nunes. *Phys. Rev. C* **72**, 017602 (2005).
- [2] M. McCleskey *et al.*, *Progress in Research*, Cyclotron Institute, Texas A&M University (2010-2011), p.I-5.
- [3] M. McCleskey *et al.*, *Progress in Research*, Cyclotron Institute, Texas A&M University (2009-2010), p.I-42.
- [4] A.M. Mukhamedzhanov, C.G. Gagliardi, and R.E. Tribble. *Phys. Rev. C* **63**, 024612 (2001).
- [5] T. Al-Abdullah *et al.*, *Phys. Rev. C* **81**, 035802 (2010).
- [6] L. Trache *et al.*, *Phys. Rev. C* **61**, 024612 (2000).
- [7] B.T. Roeder *et al.*, *Nucl. Instrum. Methods Phys. Res.* **A634**, 71 (2011).
- [8] I.J. Thompson, *Comput. Phys. Rep.* **7**, 167 (1988).
- [9] R.C. Johnson and P.J.R. Soper, *Phys. Rev. C* **1**, 976 (1970).
- [10] R.L. Varner, *Phys. Rep.* **201** (2), 57 (1991).
- [11] G.L. Wales and R.C. Johnson, *Nucl. Phys.* **A274**, 168 (1976).
- [12] C.A. Bertulani, *Comput. Phys. Commun.* **156**, 123 (2003).
- [13] A. Horvath *et al.*, *Astrophys. J.* **570**, 926 (2002).
- [14] M. Wiescher, J. Görres, and F.K. Thielemann, *Astrophys. J.* **363**, 340 (1990).
- [15] R. Reifarth *et al.*, *Phys. Rev. C* **77**, 015804 (2008).